INFECTION AND IMMUNITY, Jan. 2010, p. 210–219 Vol. 78, No. 1
0019-9567/10/$12.00 doi:10.1128/IAI.00864-09

Roles of Capsule and Lipopolysaccharide O Antigen in Interactions of Human Monocyte-Derived Dendritic Cells and *Klebsiella pneumoniae*[▽]

B. Evrard,[1,2]* D. Balestrino,[3] A. Dosgilbert,[1] J.-L. J. Bouya-Gachancard,[2] N. Charbonnel,[3] C. Forestier,[3] and A. Tridon[1,2]

CHU Clermont-Ferrand, Laboratoire d'Immunologie, Clermont-Ferrand, France[1]; Université d'Auvergne-Clermont 1, UFR Médecine-Pharmacie, Laboratoire d'Immunologie, Clermont-Ferrand, France[2]; and Université d'Auvergne-Clermont 1, UFR Pharmacie, Laboratoire de Bactériologie, Clermont-Ferrand, France[3]

Received 31 July 2009/Returned for modification 5 September 2009/Accepted 11 October 2009

In humans, *Klebsiella pneumoniae* is a saprophytic bacterium of the nasopharyngeal and intestinal mucosae that is also frequently responsible for severe nosocomial infections. Two major factors of virulence, capsular polysaccharide (CPS) and lipopolysaccharide (LPS) O antigen, are involved in mucosal colonization and the development of infections. These bacterial surface structures are likely to play major roles in interactions with the mucosal immune system, which are orchestrated by a network of surveillance based on dendritic cells (DCs). To determine the roles of *K. pneumoniae* CPS and LPS in the DC response, we investigated the response of immature human monocyte-derived DCs to bacterial challenge with a wild-type strain and its isogenic mutants deficient in CPS or LPS O-antigen production. As observed by flow cytometry and confocal laser microscopy, the rate of phagocytosis was inversely proportional to the amount of CPS on the bacterial cell surface, with LPS playing little or no role. The *K. pneumoniae* wild-type strain induced DC maturation with upregulation of CD83, CD86, and TLR4 and downregulation of CD14 and DC-SIGN. With CPS mutants, we observed a greater decrease in DC-SIGN, suggesting a superior maturation of DCs. In addition, incubation of DCs with CPS mutants, and to a lesser extent with LPS mutants, resulted in significantly higher Th1 cytokine production. Combined, our findings suggest that *K. pneumoniae* CPS, by hampering bacterial binding and internalization, induces a defective immunological host response, including maturation of DCs and pro-Th1 cytokine production, whereas the LPS O antigen seems to be involved essentially in DC activation.

Klebsiella pneumoniae is a Gram-negative enterobacterium ubiquitous in nature with two classical habitats, the environment (surface waters, vegetation, and soil) and the mucosal surfaces of mammals (32). In humans, *K. pneumoniae* behaves like a saprophyte mainly in the nasopharyngeal and intestinal mucosae. It is an opportunistic bacterium frequently involved in severe nosocomial infections in immunocompromised patients, mainly pneumonia, urinary tract infections, and bacteremia (4, 23). In the absence of treatment, *K. pneumoniae* infections have a high rate of mortality. In addition, the emergence of multi-antibiotic-resistant *K. pneumoniae* in nosocomial strains has underlined the need for a fundamental understanding of the immunological mechanisms of *K. pneumoniae* infections to develop new approaches to treatment, such as vaccination or immunotherapy (29, 31, 32).

K. pneumoniae has two major virulence factors, capsular polysaccharide (CPS) and lipopolysaccharide (LPS). CPS is a voluminous outer layer and is involved in protection against C3 deposition that occurs mainly in the inhibition of macrophage phagocytosis (2, 13). LPS comprises three parts, lipid A, core, and O antigen, which is the outermost component and is a polysaccharidic side chain. O antigen is responsible for the resistance of bacteria to complement-mediated killing (1, 28). Both components are essential to the blood passage of bacteria and to the development of sepsis, but only CPS is involved in the development of *K. pneumoniae* pulmonary infections (13).

The initial interaction between bacteria and the host mucosal immune system probably occurred through recognition between these surface components and dendritic cells. Indeed, the mucosal immune response is orchestrated by a network of surveillance based on dendritic cells (DCs), which are professional antigen-presenting cells (10, 21, 33). Immature DCs reside in peripheral tissues, especially in mucosal membranes, such as the gut or lung mucosae. They sense the microenvironment and have a great ability to detect, take up, and process antigens. Antigenic stimulation triggers a DC maturation process with upregulation of membrane molecules (CD80, CD86, CD83, HLA-DR, and CD40) and cytokine production. The modulation of DC activation by the local cytokine microenvironment and by pattern recognition receptors (PRRs) induces differential subsets of DCs. The DC subsets secondarily determine different effector responses of the T cells, Th1, Th2, regulatory T cells, and Th17 (27). PRRs include toll-like receptors (TLRs) and C-type lectin receptors (CLRs) and recognize danger signals, such as pathogen-associated molecular patterns (PAMPs), including the LPS of Gram-negative bacteria (37). TLR4 is a membrane toll-like receptor that is, in association with its coreceptor CD14, the central protein involved in the response of Gram-negative bacteria by LPS recognition, cell signaling, and NF-κB-mediated production of cytokines (19). Within the CLR family, DC-SIGN is an endocytic receptor involved in the internalization of Gram-negative

* Corresponding author. Mailing address: Laboratoire d'Immunologie, Hôtel-Dieu, Boulevard Leon Malfreyt, F-63058 Clermont-Ferrand, France. Phone: 33 4 73 750 662. Fax: 33 4 73 750 637. E-mail: bevrard@chu-clermontferrand.fr.

▽ Published ahead of print on 19 October 2009.

TABLE 1. Bacterial strains and primers

K. pneumoniae strain/primer	Description	Source or reference
LM21	Clinical isolate; serogroup O2ab; ApR	16
LM21 *gfp*	LM21 strain SHV-1::*aadA7-gfpmut3* Sp^r	3
LM21-Δ*wzm*	LM21 SHV-1::*aadA7-gfpmut3* Δ*wzm*::GB Km^r Sp^r	3
LM21-Δ*wbbM*	LM21 SHV-1::*aadA7-gfpmut3* Δ*wbbM*::GB Km^r Sp^r	3
LM21-Δwza (ΔORF4)	LM21 SHV-1::*aadA7-gfpmut3* ΔORF4::GB Km^r Sp^r	3
LM21-Δwzx (ΔORF14)	LM21 SHV-1::*aadA7-gfpmut3* ΔORF14::GB Km^r Sp^r	3
LM21-Δ*wecA*	LM21 SHV-1::*aadA7-gfpmut3* Δ*wecA*::GB Km^r Sp^r	This study
wecA.GB-5′	CTGGAGTTGGGGCATCATCGCTATACTTCCCGGATTAACT ATGCTGAGAGCACATGCGTTAAAGCCACGTTGTGTCTCAA	This study
wecA-GBnp-3′	CTACTTGGTTAGTTTCGGATTATTGCCGCTGTGTCGCCGAA TTCTGCGTCTATGCGCTTTTAGAAAAACTCATCGAGCA	This study

bacteria (48). It modulates TLR4-induced maturation by enhancing IL-10 production and inhibiting Th1 polarization (14, 17, 42, 43).

The role of DCs in the development of *K. pneumoniae* infections has not yet been clearly elucidated. DCs are a critical component of early lung inflammation elicited in a murine *K. pneumoniae* infection model and play a role in regulating lung barrier integrity (45). In another murine model of invasive bacterial pneumonia, it has been shown that DCs expressing TLR9 are required for effective innate immune response against *K. pneumoniae*, in particular to allow functional activation of lung macrophages and NK and T cells (5). In humans, little is known about the contribution of DCs to the host response to *K. pneumoniae* infections. Only in vitro experiments have been performed, and they indicate that *K. pneumoniae* induces maturation of immature human DCs and production of interleukin 12 (IL-12) (7).

This article investigates the effects of a clinical isolate of *K. pneumoniae*, LM21 (16), on immature human monocyte-derived DCs (mo-DCs). The aim was to compare the internalization ability and the bacterium-induced specific phenotype of mo-DCs using the *K. pneumoniae* LM21 wild-type strain and its isogenic mutant strains deficient in LPS or CPS synthesis in order to determine the respective roles of CPS and LPS O antigen in the DC response to bacteria.

MATERIALS AND METHODS

Bacterial strains and culture conditions. The bacterial strains used in this study are shown in Table 1. The green fluorescent protein (GFP)-tagged *K. pneumoniae* wild-type strain and its isogenic Δ*wzx*, Δ*wza*, Δ*wbbM*, and Δ*wzm* mutants were previously constructed by integrating an *aadA7-gfpmut3* cassette into the $bla_{SHV\text{-}1}$ β-lactamase-encoding gene (chromosomal ampicillin resistance) (3). A Δ*wecA* mutant was constructed using the same strategy and the specific primers shown in Table 1. All bacterial strains were stored at −20°C and −80°C in lysogeny broth (LB) medium containing 15% glycerol. Antibiotics were added to the media for appropriate bacterial strains at the following concentrations: ampicillin, 50 $\mu g \cdot ml^{-1}$; kanamycin, 50 $\mu g \cdot ml^{-1}$. Bacterial growth was monitored by measuring the optical density at 620 nm (OD_{620}).

Extraction and analysis of bacterial exopolysaccharides (CPS and LPS). Capsular polysaccharides were extracted from a bacterial culture grown overnight in M63B1-0.4% glucose medium. Capsular polysaccharides were extracted according to the method previously described by Domenico et al. (15) and quantified by measuring uronic acid (6). LPS was extracted from *K. pneumoniae* cells grown in LB using an LPS extraction kit (Intron Biotechnology). LPS samples were separated by Tricine–SDS-PAGE and visualized by silver staining with the SilverXpress silver-staining protocol (Invitrogen).

Microscope observations. For scanning electron microscopy (SEM) and transmission electron microscopy (TEM), bacteria were fixed for 18 h at 4°C with a fixation solution containing (vol/vol) 4% glutaraldehyde in water, 0.15% ruthenium red in water, and 0.2 M cacodylate buffer (pH 7.4). After three washes with the same solution without glutaraldehyde, samples were postfixed in 1% OsO_4 in cacodylate buffer for 1 h. All samples were then dehydrated with a graded series of ethanol. SEM was performed on biofilms grown on Thermanox slides (Nalgene) attached to the internal removable glass slide of the microfermentors or deposited on a well bottom of a 24-well plate (Nunc). For TEM, dried samples were embedded in a polymerized 2-mm-thick Epon coating, and ultrathin sections were picked up with Formvar-coated copper grids (300 mesh). The sections were counterstained with 4% aqueous uranyl acetate. For negative staining, bacteria were grown overnight in M63B1-0.4% Glu medium and negatively stained with 2% phosphotungstic acid on Formwar-coated copper grids (300 mesh) (Electron Microscopy Sciences, Hatfield, PA).

In vitro differentiation of monocyte-derived dendritic cells. Mo-DCs were generated from peripheral blood mononuclear cells (PBMCs). Briefly, PBMCs were isolated from the buffy coats of healthy volunteers obtained from the local French blood agency (Etablissement Français du Sang of Saint-Etienne) by Ficoll-Histopaque (Sigma, Saint-Quentin Fallavier, France) density gradient centrifugation. The PBMCs were washed twice with RPMI 1640 (Cambrex Bio Science, Verviers, Belgium), and the monocytes were then isolated by adherence (2 h). Surface plates (75-cm^2 flasks; BD Falcon, Le Pont de Claix, France) were precoated with 1 μg/ml poly-L-lysine (PLL) (Sigma) for 2 h at 4°C. The monocytes were then cultured for 5 days in RPMI 1640 supplemented with 1% L-glutamine (Sigma), 10% fetal calf serum (FCS), and 0.5% penicillin-streptomycin (Sigma) containing 500 U/ml IL-4 (R&D Systems, Lille, France) and 800 U/ml granulocyte-macrophage colony-stimulating factor (GM-CSF) (R&D Systems). After 3 days of incubation, one-half volume of fresh medium containing 2× doses of IL-4 and GM-CSF was added to each well.

Binding assay. On day 6, immature DCs were plated in 12-well plates and suspended in RPMI 1640 with 10% FCS at a concentration of 1×10^5 cells/ml. The cells were incubated at 37°C in the presence of 5% CO_2 with the GFP-tagged *K. pneumoniae* wild-type strain or its mutants to a range of final concentrations of 10^3 to 10^8 CFU/ml, i.e., a bacterium/DC ratio of 1:100 to 1,000:1, respectively. At different times, ranging from 0 h to 5 h, immature DCs were washed once to remove unbound bacteria. A 1:4 dilution of trypan blue (0.4%; Sigma) was added to the cells for 5 min to quench the fluorescence from extracellular labeled bacteria. The cells were then analyzed by flow cytometry and gated to large cells, thereby excluding unbound bacteria from the analysis. Binding was determined by comparing the percentage of fluorescence-positive DCs with the whole DC population.

Confocal microscopy observations. Immature DCs were plated in 12-well plates and suspended in RPMI 1640 with 10% FCS at a concentration of 1×10^5 cells/ml. The cells were incubated at 37°C in the presence of 5% CO_2 with the UV-killed GFP-labeled *K. pneumoniae* (10^8 CFU/ml). After 2 h of incubation, the cells were washed with phosphate-buffered saline (PBS), and 50 μl was allowed to adhere to coverslips. The cells were fixed with paraformaldehyde (4%) for 15 min at room temperature and were permeabilized in a solution of 0.1% saponin for 15 min at room temperature. The preparations were stained with a mouse monoclonal anti-DC-SIGN antibody (clone 120507; 20 μg/ml; R&D Systems), followed by incubation with Cy3-labeled goat anti-mouse antibody diluted 1/1,000 in PBS, and kept at 4°C until they were processed for microscopy analysis. The coverslips were mounted in fluorescent mounting medium (a 1:3 solution of glycerol-PBS). All samples were imaged using an oil immersion objective (40×) on a Zeiss LSM 510 confocal laser scanning micro-

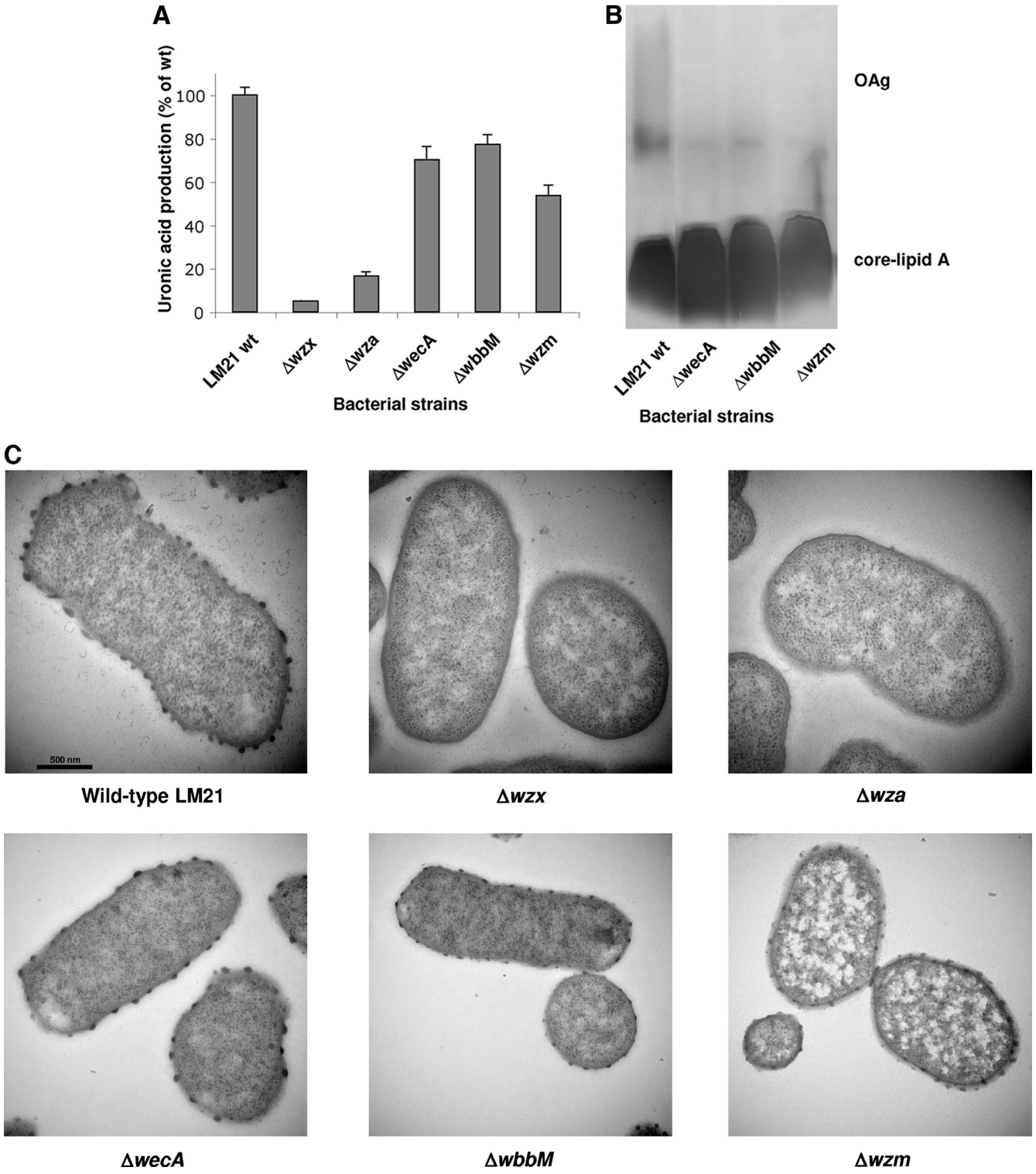

FIG. 1. Characterization of the surface layers of *K. pneumoniae* mutant strains. (A) Quantification of uronic acid production was determined with *K. pneumoniae* wild-type (wt) and exopolysaccharide-deficient isogenic mutants (Δ*wzx*, Δ*wza*, Δ*wzm*, Δ*wbbM*, and Δ*wecA*). Measurements were made of bacteria cultivated for 18 h in M63B1-0.4% Glu medium, and the results are expressed as percentages of the uronic acid production by the wild-type LM21 strain, set at 100%. The data are means plus standard errors of the means of three separate experiments. (B) LPS preparations from the *K. pneumoniae* wild type and the Δ*wzm*, Δ*wbbM*, and Δ*wecA* mutants. Extracts were separated by Tricine–SDS-PAGE and visualized by silver staining. Ag, antigen. (C and D) Surface-expressed CPS was evident for the wild-type strain and the Δ*wecA*, Δ*wbbM*, and Δ*wzm* mutants as electron-dense material on the surfaces of whole cells examined by transmission electron microscopy (C) and as thin threads emerging from the bacterial body surface by scanning electron microscopy (D).

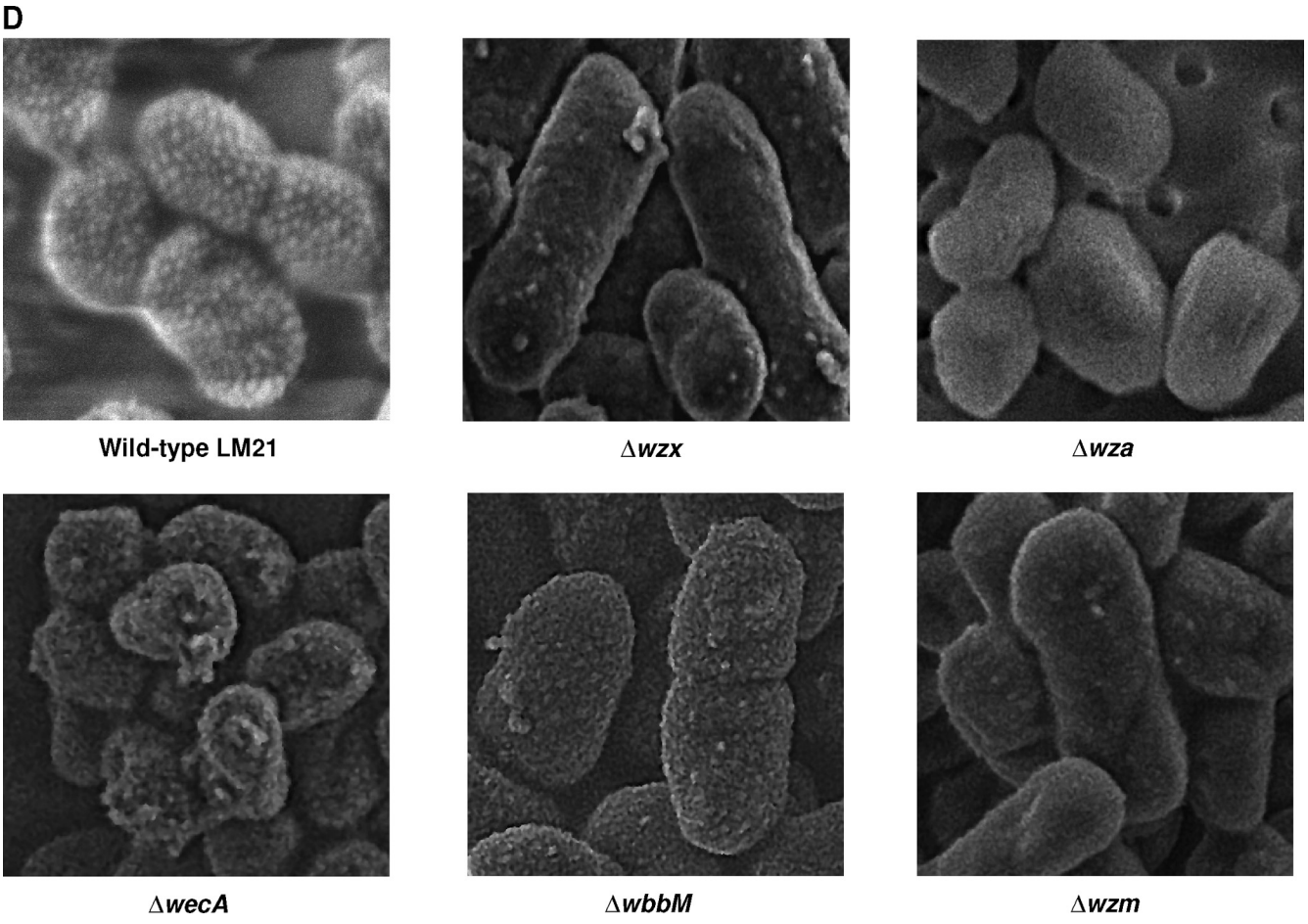

FIG. 1—*Continued.*

scope from the Centre d'Imagerie Cellulaire Santé (CICS), Université d'Auvergne-Clermont 1. The detector filter bandwidths were selected to ensure no cross-bleeding from one channel into another. Single-color controls were included in experiments to confirm the settings on the confocal microscope. Images were analyzed using Zeiss LSM Image Browser microscope software.

Maturation of DCs in the presence of *K. pneumoniae* and analysis by flow cytometry. On day 6, the immature DCs from each well were harvested, pooled, centrifuged, and reseeded in 12-well plates (Becton Dickinson, Le Pont de Claix, France) at 1×10^5 cells/ml. UV-killed bacteria were then added as 10 μl medium per well to a range of final concentrations of 10^3 to 10^7 CFU/ml, i.e., a bacterium/DC ratio of 1:100 to 100:1, respectively. LPS from *Escherichia coli* (Sigma, Saint Quentin Fallavier, France) at a final concentration of 100 ng/ml was used as a positive control. Immature dendritic cells without the addition of LPS or bacteria were used as a negative control. The cells were incubated for 48 h at 37°C in a 5% CO_2 atmosphere.

On day 8, the cells were collected, centrifuged, and resuspended in PBS. To block nonspecific binding of antibody reagents, 1% bovine serum albumin (BSA) (Sigma) was added to the PBS. Subsequently, one-third of the volume was incubated for 30 min at 4°C with a cocktail of five antibodies (1 μl/100,000 cells for each antibody). Murine antibodies against human CD14, CD86, CD83, DC-SIGN (CD209), and TLR4 (biotin antibody) were used, coupled with allophycocyanin (APC)-Cy7, phycoerythrin (PE), fluorescein isothiocyanate (FITC), peridinin chlorophyll protein (PerCP)-Cy5.5, and APC (streptavidin APC), respectively. All antibodies were obtained from BD Biosciences (Le Pont de Claix, France). One-third of the volume was incubated with the five corresponding murine isotype-matched control antibodies (BD Biosciences), and one-third was used as an unlabeled control. The cells were analyzed using BD-LSRII with FACSDiva Software (BD Biosciences) from the CICS. Compensation fluorescence adjustments were performed. Gates were set on living DCs based on forward/side scatter properties. The analysis was based on a count of 3,000 DCs. The level of staining was expressed as the mean fluorescence intensity (MFI). Each experiment was performed at least four times.

Cytokine quantification. Cytokines (IL-10 UltraSensitive, IL-12, and tumor necrosis factor alpha [TNF-α]), were measured in culture supernatants from DC culture media using enzyme-linked immunosorbent assay (ELISA) kits (Biosource, Nivelles, Belgium) according to the manufacturer's instructions.

Statistical analysis. Student's matched-pairs *t* test was used to compare means. *P* values lower than 0.05 were considered statistically significant. Correlations were evaluated by Pearson's coefficient (ρ).

RESULTS

Characterization of *K. pneumoniae* mutants. To assess the precise role of exopolysaccharides in the interaction with DCs, we used four previously characterized *K. pneumoniae* isogenic allelic-exchange mutants: Δ*wza* (open reading frame 4 [ORF4]; transport of capsular polysaccharides), Δ*wzx* (glycosyl transferase; capsule biosynthesis), Δ*wzm* (LPS transport pathway), and Δ*wbbM* (LPS biosynthesis) (3). A fifth mutant was constructed by specific deletion of the *wecA* gene, since it had been previously shown that a *K. pneumoniae wecA* mutant fails to produce the O antigen but produces a wild-type level of capsular polysaccharides (26). A notable and significant deficiency in uronic acid production—a significant constituent of the *K. pneumoniae* capsule—in the Δ*wza* and Δ*wzx* mutants confirmed the gene disruptions (Fig. 1A). However, measurement

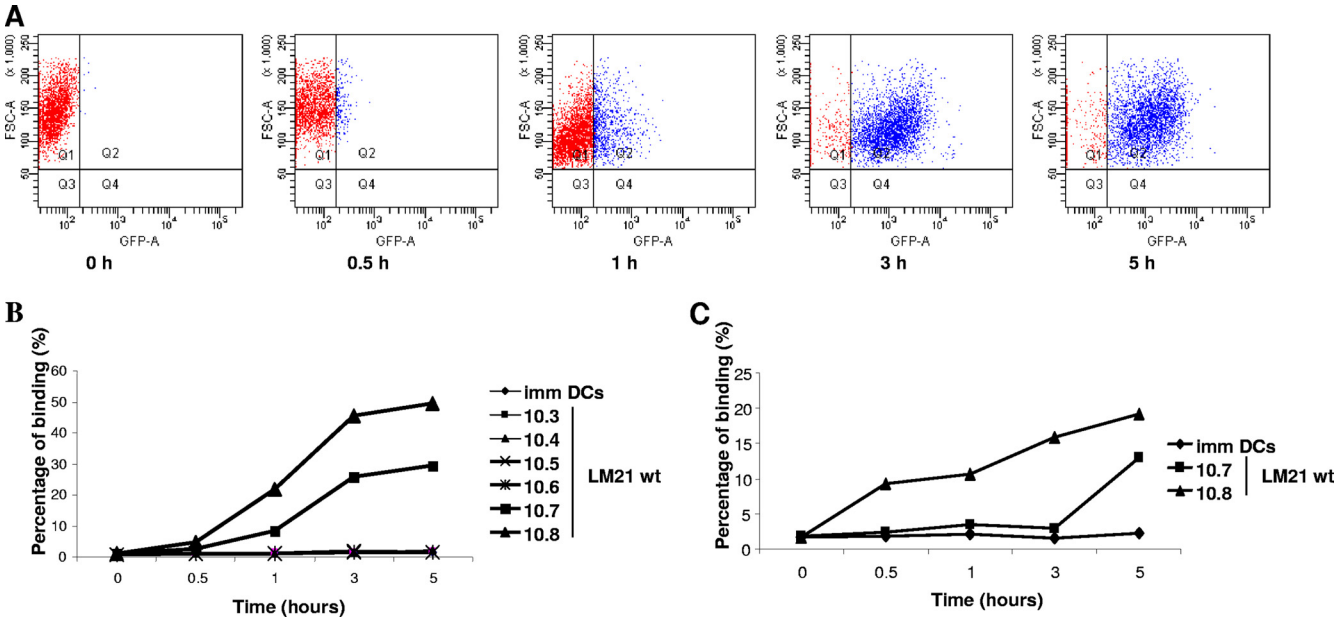

FIG. 2. Kinetics of *K. pneumoniae* wild-type strain LM21 binding to human mo-DCs. (A) Data from a representative experiment. Shown are forward scatter (FSC)/GFP dot plots gated on human mo-DCs incubated with 1×10^8 CFU/ml GFP-tagged *K. pneumoniae* wild-type strain. After several incubations, nonadherent bacteria were removed by washing them, and binding was determined by comparing the percentage of fluorescence-positive DCs (Q2) with that of the whole DC population (Q1 + Q2). (B and C) Human mo-DCs were incubated with a range of bacterial cells, live (B) or previously UV killed (C). The data are the means of 10 independent experiments. imm DCs, immature DCs; LM21 wt, DCs matured with LM21 wild-type *K. pneumoniae* at different concentrations.

of uronic acid production in the *K. pneumoniae* LM21 Δ*wecA*, Δ*wbbM*, and Δ*wzm* mutants showed lower levels than those of the parental strain, indicating that the main capsule component synthesis was also impaired, albeit slightly, in these mutants (Fig. 1A), probably owing to overlaps between the LPS-biosynthetic and capsule production pathways. TEM with negatively stained bacteria and SEM observations confirmed these results and showed a drastic reduction in capsule production in the Δ*wzx* and Δ*wza* mutants, whereas surface-expressed CPS was evident for the three other mutants (Fig. 1C and D). Extraction of LPS, followed by gel electrophoresis, showed no or faint bands corresponding to the O antigen with the extracts of the Δ*wecA*, Δ*wbbM*, and Δ*wzm* mutants compared to that of the wild-type strain (Fig. 1B).

Phagocytosis of *K. pneumoniae* wild-type strain LM21 by human mo-DCs. To determine the capacity of the human mo-DCs to phagocytize encapsulated *K. pneumoniae* wild-type strain, cells were incubated with a broad range of live bacteria and binding was analyzed by flow cytometry (Fig. 2A and B). With concentrations ranging from 10^3 to 10^6 CFU/ml, i.e., a bacterium/DC ratio of 1:100 to 10:1, respectively, no binding of the bacteria to DCs was detected during the 5 h of the experiments. Conversely, at concentrations of 10^7 CFU/ml and 10^8 CFU/ml, i.e., a bacterium/DC ratio of 100:1 to 1,000:1, respectively, binding of the GFP-labeled bacteria was detected in the first half hour and gradually increased over time to reach maximums of 29.6% and 49.5%, respectively, at 5 h. When the same experiments were performed with previously UV-killed bacterial cells, the same results were obtained with slower kinetics up to a maximum of 12.9% and 19.2%, respectively (Fig. 2C). To determine if human mo-DCs were able to internalize the bacteria and not only to bind them, laser scanning confocal microscopy was performed. After three-dimensional reconstruction, it confirmed that bacteria were localized within the mo-DCs (Fig. 3A).

Roles of CPS and LPS O antigen in phagocytosis by human mo-DCs. To investigate the respective roles of CPS and LPS O antigen in bacterial phagocytosis by human mo-DCs, we compared the abilities of both live and UV-killed *K. pneumoniae* CPS or LPS mutants to bind immature mo-DCs to that of their parental wild-type strain (Fig. 3B). We chose to assess binding at 3 h in order to objectify wide variations. As expected, the unencapsulated mutants, Δ*wzx* and Δ*wza*, showed strongly increased binding to human mo-DCs, confirming that the presence of a capsule reduced bacterial phagocytosis. Binding of the Δ*wzx* mutant, whose CPS synthesis is strongly impaired, was systematically faster than Δ*wza* mutant binding and reached 100% even with UV-killed bacteria. The bacterium/DC binding with the three LPS O-antigen mutant strains, Δ*wecA*, Δ*wbbM*, and Δ*wzm*, was lower than that observed with the unencapsulated mutants, although higher than with the wild-type strain. In addition, binding of Δ*wzm* bacterial cells, the LPS mutant with the lowest production of CPS (50% of the wild-type CPS expression), was distinctly higher than that of the other two LPS mutants. Using UV-killed bacteria, the overall profiles of internalization of the different strains were the same, with weaker percentages. With both live and UV-killed bacteria, very high Pearson's correlation coefficients between the uronic acid measurement and rate of internalization were obtained: $\rho = -0.96$ and -0.93, respectively. Thus, the rate of internalization seemed to be inversely proportional to the amount of CPS on the bacterial cell surface, with LPS

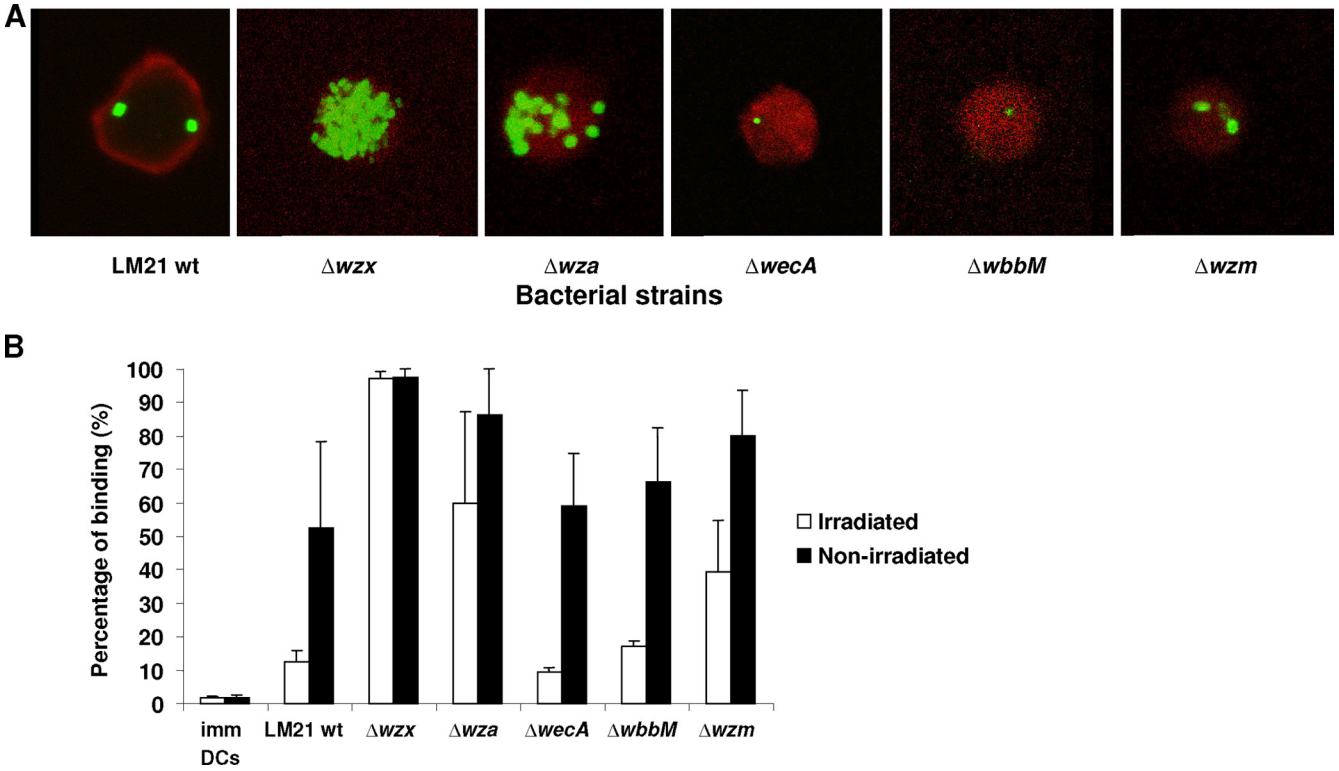

FIG. 3. Comparison of phagocytosis of *K. pneumoniae* wild-type strain LM21 and its derived isogenic mutants by human mo-DCs. (A) Confocal microscopy of LM21 wild-type strain GFP-*K. pneumoniae* cells and its derived isogenic mutants phagocytosed by a human mo-DC. The images were obtained after 2 h of incubation with 1×10^8 CFU/ml of bacteria. (B) Human mo-DCs were incubated with bacterial cells (1×10^8 CFU/ml) previously UV killed or not. After 3 h of incubation, nonadherent bacteria were removed by washing them, and bound bacteria were quantified. The number of cells with associated bacteria is presented as a percentage of the whole DC population. The data are the means and standard deviations of four independent experiments.

playing little or no role. Three-dimensional reconstruction using confocal laser scanning microscopy confirmed that bacteria were within mo-DCs. The number of bacteria present within each mo-DC was then determined (Fig. 3A). The wild-type strain was observed with a number of bacteria in each mo-DC, ranging from 0 to 3, with an average of 0.9 bacteria per cell. It ranged from 4 to more than 50 for the Δ*wzx* mutant (an average of 30.3 bacteria per cell), from 0 to 25 for the Δ*wza* mutant (an average of 8.1 bacteria per cell), from 0 to 8 for the Δ*wecA* mutant (an average of 1.1 bacteria per cell), from 0 to 2 for the Δ*wbbM* mutant (an average of 0.6 bacteria per cell), and from 0 to 20 for the Δ*wzm* mutant (an average of 3.7 bacteria per cell). Compared to the wild-type strain, the number of bacteria per cell was much greater for unencapsulated mutants, was only slightly higher for the Δ*wzm* mutant, and was not affected for the other two LPS mutants (Δ*wecA* and Δ*wbbM*).

***K. pneumoniae* wild-type strain LM21 modulates the phenotype of human mo-DCs and induces maturation.** The expression of CD83, CD86, CD14, DC-SIGN, and TLR4 was detected by flow cytometry on the surfaces of mo-DCs exposed to either the wild-type *K. pneumoniae* strain or its CPS- and LPS-deficient mutants. As expected, on day 8, immature DCs were characterized by high levels of DC-SIGN expression, with low expression of CD86 and CD14 (CD14 expression was compared to the initial expression on monocytes before the differentiation of DCs) (Fig. 4A and data not shown). Mature LPS-induced DCs expressed the converse phenotype, with a very high level of CD86 expression and a decreased level of DC-SIGN and CD14 (Fig. 4A). DC-SIGN (CD209) is a CLR family member, specific to immature DCs and classically downregulated during maturation, whereas CD86 is a costimulatory molecule that is upregulated during DC maturation and CD14 is a coreceptor of LPS, a molecule specific to monocytes that is downregulated during differentiation into DCs.

We also assessed DC maturation after 48 h of incubation with a range of UV-killed *K. pneumoniae* wild-type strain LM21 bacteria, with bacterial concentrations ranging from 10^3 to 10^7 CFU/ml, i.e., bacterium/DC ratios of 1:100 to 100:1, respectively (Fig. 4A). Upon maturation, *K. pneumoniae* induced a dose-dependent higher expression of CD86 and a dose-dependent lower expression of DC-SIGN (Fig. 4A). The induced phenotype was thus very similar to that of mature LPS-induced DCs. At 1×10^3 CFU/ml, CD86 and DC-SIGN were slightly modified, reflecting very early activation, which increased at higher bacterial concentrations and reached a plateau at 1×10^5 CFU/ml. There was no significant variation in the CD14 MFI whatever the bacterial concentration. For markers with lower cell surface density, such as CD83, a marker specific to mature DCs, and TLR4, an LPS receptor with activation functions, *K. pneumoniae* also induced a dose-dependent higher expression, and the phenotypes obtained

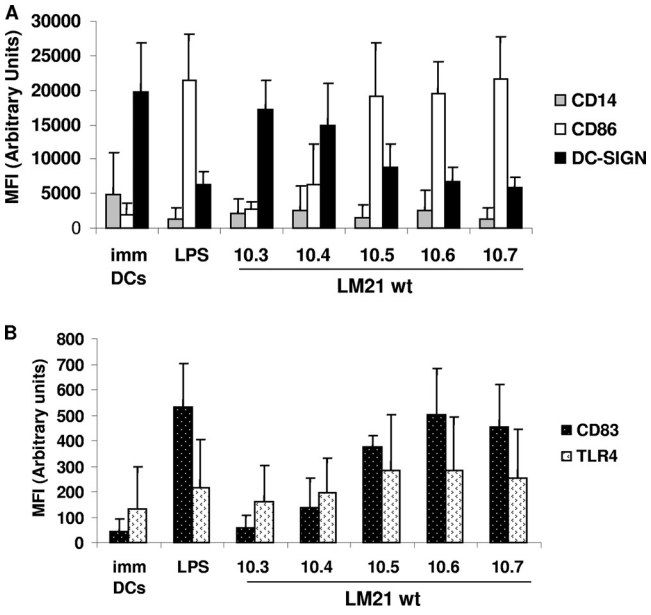

FIG. 4. Maturation of human mo-DCs after exposure to a range of *K. pneumoniae* wild-type strains. The histograms show MFI values on gated DCs. (A) Differential expression on DCs of high-density surface molecules: CD86, DC-SIGN, and CD14. *K. pneumoniae* induced a dose-dependent higher expression of CD86 and a dose-dependent lower expression of DC-SIGN compared to immature DCs. (B) Differential expression on DCs of low-density surface molecules: TLR4 and CD83. *K. pneumoniae* induced a dose-dependent higher expression of CD83 and TLR4 compared to immature DCs. The data presented correspond to the means and standard deviations of the MFIs of five (A) and four (B) representative experiments. Isotypic control values were always subtracted from the MFI of each marker. LPS, DCs matured with extracts of *E. coli* LPS.

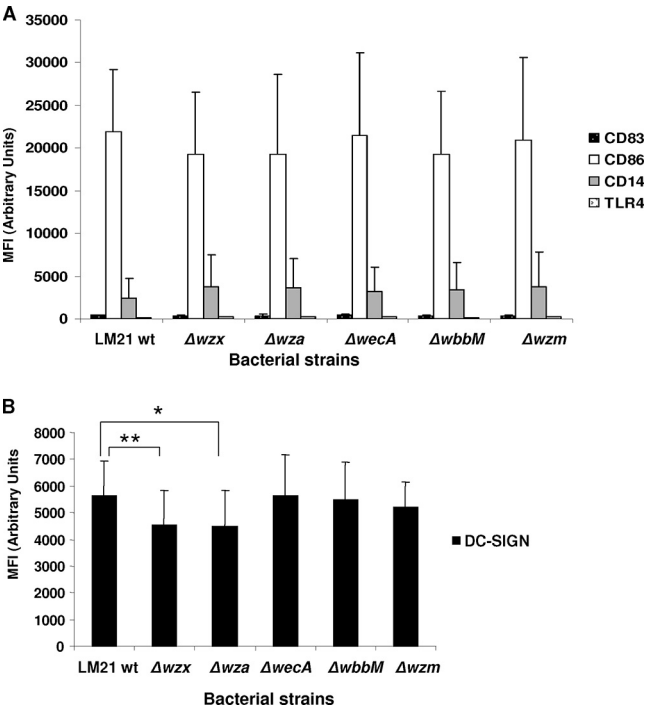

FIG. 5. Maturation of human mo-DCs after exposure to 1×10^5 CFU/ml *K. pneumoniae* wild-type strain or its derived isogenic mutants. The histograms show MFI values on gated DCs. Overall, the phenotypes induced by the different bacteria were very similar and corresponded to those of mature DCs with strongly expressed CD86 (A) and strongly decreased DC-SIGN (B) compared to immature DCs. (B) With CPS mutant strains, the decrease in DC-SIGN was significantly greater. The data presented correspond to the means and standard deviations of the MFIs in three independent experiments. Isotypic control values were always subtracted from the MFI of each marker.

were very similar to those induced by *E. coli* LPS extract. The plateau was also reached at 1×10^5 CFU/ml (Fig. 4B).

Maturation of human mo-DCs after exposure to *K. pneumoniae* CPS and LPS mutants. To determine if bacterial exopolysaccharides were involved in the DC phenotypic modifications previously observed, we assessed the expression of the same cell surface markers using isogenic CPS- or LPS-deficient mutants of *K. pneumoniae*. We chose to work with a concentration of 1×10^5 CFU/ml, because it was the lowest concentration leading to a complete maturation of DCs with the wild-type strain. Overall, the different mutant bacteria induced a phenotype of maturation similar to that of the mature DCs treated with the wild-type strain, with a highly increased expression of CD86, and to a lesser extent of CD83, and a strongly decreased expression of DC-SIGN (Fig. 5A and B). The only significant difference observed between the mutants and the wild-type strain was a small, but constant, decrease in the DC-SIGN MFI expression with the mo-DCs exposed to the two CPS mutants, Δ*wzx* ($P = 0.0046$) and Δ*wza* ($P = 0.035$) (Fig. 5B).

Cytokine production by wild-type *K. pneumoniae*- and CPS/LPS mutant-treated DCs. We first determined the effect of the incubation of immature DCs with *K. pneumoniae* wild-type strain LM21 on the production of an anti-inflammatory cytokine, IL-10, and two pro-Th1 cytokines, IL-12 and TNF-α, using UV-killed bacteria with concentrations ranging from 10^3 to 10^7 CFU/ml (Fig. 6A). Dose-dependent increases in the production of IL-12 and TNF-α were induced by the *K. pneumoniae* wild-type strain and, to a lesser extent, in the production of IL-10. We next examined whether the differences in the interactions of DCs with the *K. pneumoniae* wild-type strain and its isogenic mutants were reflected in functionally distinct cytokine profiles (Fig. 6B). As for the cytometry results, we chose to work at 10^5 CFU/ml. Compared to the wild-type strain, with the Δ*wzx* mutant strain, we obtained an increase in IL-12 (a 3.3-fold change; $P = 0.217$), TNF-α (a 5.2-fold change; $P = 0.111$), and IL-10 (a 2-fold change; $P = 0.035$) cytokine production. Compared to the wild-type strain, we obtained with the Δ*wza* mutant an increase in IL-12 (a 3.2-fold change; $P = 0.121$), TNF-α (a 4-fold change; $P = 0.052$), and IL-10 (a 2.4-fold change; $P = 0.105$) cytokine production. With the LPS O-antigen mutants, Δ*wec*A and Δ*wzm*, bacteria roughly doubled the production of the three cytokines compared to the wild-type strain, whereas with the Δ*wbbM* mutant, cytokine production remained similar to that of the wild-type strain.

DISCUSSION

In this study, we compared, in an in vitro model, the effect of a pathogenic encapsulated *K. pneumoniae* wild-type strain on immature DCs generated from human monocytes with that of

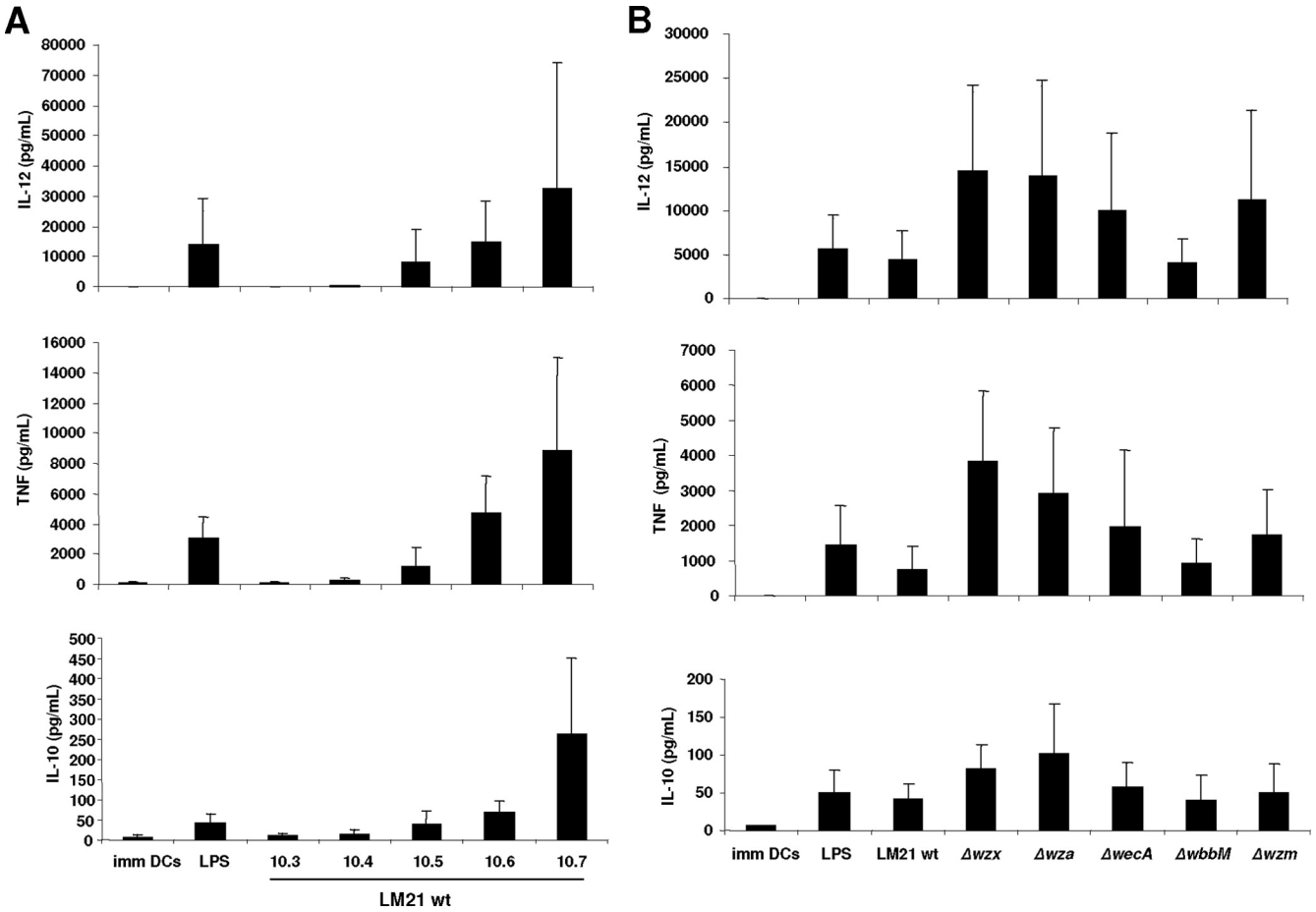

FIG. 6. (A) Cytokine production of human mo-DCs after exposure to a range of the same *K. pneumoniae* wild-type strain. *K. pneumoniae* induced dose-dependent production of IL-12, TNF-α, and IL-10. The production of IL-12 and TNF-α, pro-Th1 cytokines, was much higher than that of IL-10. (B) Differential profiles of human mo-DC cytokine production after exposure to 1×10^5 CFU/ml *K. pneumoniae* wild-type strain or its derived isogenic mutants. The data presented correspond to the means and standard deviations of four independent experiments.

its isogenic mutant strains, unencapsulated or deficient in LPS O antigen. Several studies have described the role of *K. pneumoniae* surface polysaccharides in interactions with macrophages or human epithelial cells, in which CPS seemed to impede cell association and cellular activation whereas LPS seemed to increase cell association, but little is known about interactions with human DCs (8, 12, 13, 16, 24, 34, 35, 39).

However, as antigen-presenting cells, dendritic cells have direct contact with bacteria coming from the environment in the different mucous membranes and play a major role in both the initiation and orientation of adaptive immune responses. In the intestinal tract, where *K. pneumoniae* finds a natural habitat, DCs in the lamina propria extend their dendrites into the intestinal lumen and continuously sample foreign antigen, including bacteria (30, 36). Subepithelial intestinal DCs are strategically located to encounter bacteria after their passage through M cells (11, 25, 41). Within the conducting airways, where *K. pneumoniae* infections develop, airway mucosal DCs also send up their dendrites into the airway lumen and take up inhaled antigen. In contrast, in the alveolar space in lung tissue, lung parenchymal DCs are present and cooperate with alveolar macrophages and T cells to develop the immune response (20, 22, 44).

Here, we demonstrated that human mo-DCs, which are functionally related to immature mucosal DCs (9, 40), were able to internalize encapsulated *K. pneumoniae* wild-type bacteria, but in a very inefficient way and only with high bacterium/DC ratios. Several reports indicate that for unencapsulated Gram-negative bacteria internalization clearly occurs more quickly despite lower bacterial concentrations. Indeed, 92% of DCs had internalized unencapsulated *Salmonella enterica* serovar Typhimurium after only 30 min of incubation (18). We previously showed, using an *E. coli* strain (personal data), that 96% of DCs with internalized bacteria were observed after 1 h of incubation (for 10^8 CFU/ml of nonirradiated *E. coli*).

In our model, capsule-deficient *K. pneumoniae* mutants were internalized by the DCs much faster than the LPS mutants, which themselves were internalized faster than the wild-type encapsulated strain. We observed an inversely proportional relationship between CPS expression (quantified by measuring uronic acid) and the rate of internalization, showing that CPS acted as a great brake on the phagocytosis of *K. pneumoniae* by

human DCs. In our study, the CPS expression of LPS mutants was partially affected, probably owing to overlaps in the mutants' biosynthesis pathways. The role of LPS in the internalization mechanism therefore remains unclear but is probably minor compared to that of CPS. Indeed, the increases in internalization obtained with LPS mutant strains were very low compared to those of CPS mutant strains. In agreement with these results, Cortés et al. reported higher phagocytic rates of a *K. pneumoniae* CPS mutant strain using human alveolar macrophages (13). Conversely, they described an LPS O-antigen Δ*wbbM* mutant strain, with no decreased CPS expression, that did not alter phagocytosis compared to the wild-type strain.

Like Braat et al., we found an increase in CD83 and CD86 expression on DCs induced by a wild-type *K. pneumoniae* strain (7). This reflects the increased costimulating capacity of DCs and therefore the greater stimulating capacity of T cells. We also studied the membrane expression of two main pattern recognition receptors, TLR4 and DC-SIGN. TLR4 is implicated in LPS recognition, cell signaling, and NF-κB-mediated production of cytokines (19), whereas DC-SIGN is a CLR, with endocytic functions, involved in the modulation of TLR4-induced maturation by enhancing IL-10 production and inhibiting Th1 polarization (14, 17, 42, 43). As we obtained the upregulation of TLR4 after DC incubation with *K. pneumoniae* bacteria, it is likely that matured DCs reached a new state, more ready to sense infection. In support of these results, it was shown recently that airway epithelial cells upregulate TLR4 expression in response to *K. pneumoniae* infection, which results in enhancement of the inflammatory response (34). Elevated levels of TLR4 on DCs and epithelial cells, acting in a coordinated manner upon *K. pneumoniae* infection, could thus trigger a powerful immune response. This hypothesis is strengthened by the recent data of Wu et al., who reported that TLR4 is involved in host recognition of *K. pneumoniae* in macrophage cell lines (46). In their study, the wild-type *K. pneumoniae* induced downregulation of DC-SIGN. Because of the functions previously described for DC-SIGN, this downregulation could reflect decreased capacities for internalization of *K. pneumoniae*-matured DCs, which is recognized to be a reflection of a mature state of DCs.

The membrane phenotypes induced by mutants were very similar to those obtained with the wild-type strain, namely, a phenotype of mature DCs. However, with CPS-deficient mutants, we observed a significant decrease in the DC-SIGN MFI compared to that obtained with the wild-type strain, reflecting better maturation of DCs and demonstrating the inhibitory role of the capsule in the early immune response.

In our model, the cytokine production of *K. pneumoniae*-matured DCs was far greater than that of immature DCs, with high IL-12 and TNF-α production compared to that of IL-10. We concluded that DC maturation with *K. pneumoniae* induced a pro-Th1 cytokine phenotype. Interestingly, we noted that the Th1 cytokine production of the two CPS mutants (Δ*wzx* and Δ*wza*) was significantly higher than that of the wild-type strain, suggesting that in the absence of capsule layer, the bacterial cell surface components have stronger effects on activating DCs to secrete cytokines. This observation, combined with the decrease in DC-SIGN previously observed, confirmed that *K. pneumoniae* CPS can impair the host immune response, probably allowing the bacteria to avoid the host defense and thus to multiply more easily. Yoshida et al. previously found that deletion of CPS increases the levels of TNF-α and IL-6 in bronchoalveolar lavage fluid of mice infected with *K. pneumoniae* strains, thus allowing a more efficient immune response and a decrease in murine mortality (47). In view of our results, we hypothesize that, in their model, lung DCs are involved in the increase in cytokine production observed with the unencapsulated strain. The role of the LPS O side chain in bacterium-cell interactions and cytokine production still remains unclear. However, for mo-DCs exposed to LPS-deficient mutants, in particular the Δ*wecA* strain, which was barely affected in CPS synthesis, a clear increase in cytokine production was observed. It is therefore likely that the LPS O antigen per se plays a specific role in DC activation.

In light of our results, it would be particularly interesting to determine whether *K. pneumoniae* constantly harbors its capsule in vivo on the mucosal surfaces or if its synthesis varies according to the bacterial environment, as suggested by some authors (38). It should then be determined whether variations in capsule synthesis are involved in a switch from a saprophytic state in healthy subjects to a pathogenic state in weakened patients.

Combined, our findings suggest that the presence of a thick capsule at the surface of *K. pneumoniae*, by blocking binding and internalization, induces a defective immunological host response, including maturation of DCs and pro-Th1 cytokine production. These results open up broader prospects, in particular an understanding of the immunological receptors underlying the internalization and activation of the cells.

ACKNOWLEDGMENTS

We thank the CICS (Centre d'Imagerie Cellulaire Santé) of Clermont-Ferrand and in particular Christelle Blavignac and Claire Szczepaniak. We also thank Sophie Coudeyras for helpful discussions and Henri Marson for his contribution to this work.

We have no conflicts of interest.

REFERENCES

1. **Albertí, S., D. Alvarez, S. Merino, M. T. Casado, F. Vivanco, J. M. Tomás, and V. J. Benedí.** 1996. Analysis of complement C3 deposition and degradation on *Klebsiella pneumoniae*. Infect. Immun. **64:**4726–4732.
2. **Alvarez, D., S. Merino, J. M. Tomás, V. J. Benedí, and S. Albertí.** 2000. Capsular polysaccharide is a major complement resistance factor in lipopolysaccharide O side chain-deficient *Klebsiella pneumoniae* clinical isolates. Infect. Immun. **68:**953–955.
3. **Balestrino, D., J. M. Ghigo, N. Charbonnel, J. A. Haagensen, and C. Forestier.** 2008. The characterization of functions involved in the establishment and maturation of *Klebsiella pneumoniae* in vitro biofilm reveals dual roles for surface exopolysaccharides. Environ. Microbiol. **10:**685–701.
4. **Bartlett, J. G., P. O'Keefe, F. P. Tally, T. J. Louie, and S. L. Gorbach.** 1986. Bacteriology of hospital-acquired pneumonia. Arch. Intern. Med. **146:**868–871.
5. **Bhan, U., N. W. Lukacs, J. J. Osterholzer, M. W. Newstead, X. Zeng, T. A. Moore, T. R. McMillan, A. M. Krieg, S. Akira, and T. J. Standiford.** 2007. TLR9 is required for protective innate immunity in Gram-negative bacterial pneumonia: role of dendritic cells. J. Immunol. **179:**3937–3946.
6. **Blumenkrantz, N., and G. Asboe-Hansen.** 1973. New method for quantitative determination of uronic acids. Anal. Biochem. **54:**484–489.
7. **Braat, H., E. C. de Jong, J. M. van den Brande, M. L. Kapsenberg, M. P. Peppelenbosch, E. A. van Tol, and S. J. van Deventer.** 2004. Dichotomy between *Lactobacillus rhamnosus* and *Klebsiella pneumoniae* on dendritic cell phenotype and function. J. Mol. Med. **82:**197–205.
8. **Clements, A., F. Gaboriaud, J. F. Duval, J. L. Farn, A. W. Jenney, T. Lithgow, O. L. Wijburg, E. L. Hartland, and R. A. Strugnell.** 2008. The major surface-associated saccharides of *Klebsiella pneumoniae* contribute to host cell association. PLoS One **3:**e3817.
9. **Cochand, L., P. Isler, F. Songeon, and L. P. Nicod.** 1999. Human lung

dendritic cells have an immature phenotype with efficient mannose receptors. Am. J. Respir. Cell Mol. Biol. **21:**547–554.
10. **Cools, N., P. Ponsaerts, V. F. Van Tendeloo, and Z. N. Berneman.** 2007. Balancing between immunity and tolerance: an interplay between dendritic cells, regulatory T cells, and effector T cells. J. Leukoc. Biol. **82:**1365–1374.
11. **Corr, S. C., C. C. Gahan, and C. Hill.** 2008. M-cells: origin, morphology and role in mucosal immunity and microbial pathogenesis. FEMS Immunol. Med. Microbiol. **52:**2–12.
12. **Cortés, G., D. Alvarez, C. Saus, and S. Albertí.** 2002. Role of lung epithelial cells in defense against *Klebsiella pneumoniae* pneumonia. Infect. Immun. **70:**1075–1080.
13. **Cortés, G., N. Borrell, B. de Astorza, C. Gómez, J. Sauleda, and S. Albertí.** 2002. Molecular analysis of the contribution of the capsular polysaccharide and the lipopolysaccharide O side chain to the virulence of *Klebsiella pneumoniae* in a murine model of pneumonia. Infect. Immun. **70:**2583–2590.
14. **den Dunnen, J., S. I. Gringhuis, and T. B. Geijtenbeek.** 2009. Innate signaling by the C-type lectin DC-SIGN dictates immune responses. Cancer Immunol. Immunother. **58:**1149–1157.
15. **Domenico, P., S. Schwartz, and B. A. Cunha.** 1989. Reduction of capsular polysaccharide production in *Klebsiella pneumoniae* by sodium salicylate. Infect. Immun. **57:**3778–3782.
16. **Favre-Bonte, S., B. Joly, and C. Forestier.** 1999. Consequences of reduction of *Klebsiella pneumoniae* capsule expression on interactions of this bacterium with epithelial cells. Infect. Immun. **67:**554–561.
17. **Geijtenbeek, T. B., S. J. Van Vliet, E. A. Koppel, M. Sanchez-Hernandez, C. M. Vandenbroucke-Grauls, B. Appelmelk, and Y. Van Kooyk.** 2003. Mycobacteria target DC-SIGN to suppress dendritic cell function. J. Exp. Med. **197:**7–17.
18. **Guo, A., M. A. Lasaro, J. C. Sirard, J. P. Kraehenbühl, and D. M. Schifferli.** 2007. Adhesin-dependent binding and uptake of *Salmonella enterica* serovar Typhimurium by dendritic cells. Microbiology **153:**1059–1069.
19. **Heumann, D., and T. Roger.** 2002. Initial responses to endotoxins and Gram-negative bacteria. Clin. Chim. Acta **323:**59–72.
20. **Holt, P. G., D. H. Strickland, M. E. Wikström, and F. L. Jahnsen.** 2008. Regulation of immunological homeostasis in the respiratory tract. Nat. Rev. Immunol. **8:**142–152.
21. **Iwasaki, A.** 2007. Mucosal dendritic cells. Annu. Rev. Immunol. **25:**381–418.
22. **Jahnsen, F. L., D. H. Strickland, J. A. Thomas, I. T. Tobagus, S. Napoli, G. R. Zosky, D. J. Turner, P. D. Sly, P. A. Stumbles, and P. G. Holt.** 2006. Accelerated antigen sampling and transport by airway mucosal dendritic cells following inhalation of a bacterial stimulus. J. Immunol. **177:**5861–5867.
23. **Jarvis, W. R., V. P. Munn, A. K. Highsmith, D. H. Culver, and J. M. Hughes.** 1985. The epidemiology of nosocomial infections caused by *Klebsiella pneumoniae*. Infect. Control. **6:**68–74.
24. **Kostina, E., I. Ofek, E. Crouch, R. Friedman, L. Sirota, G. Klinger, H. Sahly, and Y. Keisari.** 2005. Noncapsulated *Klebsiella pneumoniae* bearing mannose-containing O antigens is rapidly eradicated from mouse lung and triggers cytokine production by macrophages following opsonization with surfactant protein D. Infect. Immun. **73:**8282–8290.
25. **Kyd, J. M., and A. W. Cripps.** 2008. Functional differences between M cells and enterocytes in sampling luminal antigens. Vaccine **26:**6221–6224.
26. **Lawlor, M. S., J. Hsu, P. D. Rick, and V. L. Miller.** 2005. Identification of *Klebsiella pneumoniae* virulence determinants using an intranasal infection model. Mol. Microbiol. **58:**1054–1073.
27. **Mazzoni, A., and D. M. Segal.** 2004. Controlling the Toll road to dendritic cell polarization. J. Leukoc. Biol. **75:**721–730.
28. **Merino, S., S. Camprubí, S. Albertí, V. J. Benedí, and J. M. Tomás.** 1992. Mechanisms of *Klebsiella pneumoniae* resistance to complement-mediated killing. Infect. Immun. **60:**2529–2535.
29. **Meyer, K. S., C. Urban, J. A. Eagan, B. J. Berger, and J. J. Rahal.** 1993. Nosocomial outbreak of *Klebsiella* infection resistant to late-generation cephalosporins. Ann. Intern. Med. **119:**353–358.
30. **Niess, J. H., S. Brand, X. Gu, L. Landsman, S. Jung, B. A. McCormick, J. M. Vyas, M. Boes, H. L. Ploegh, J. G. Fox, D. R. Littman, and H. C. Reinecker.** 2005. CX3CR1-mediated dendritic cell access to the intestinal lumen and bacterial clearance. Science **307:**254–258.
31. **Paterson, D. L., W. C. Ko, A. Von Gottberg, S. Mohapatra, J. M. Casellas, H. Goossens, L. Mulazimoglu, G. Trenholme, K. P. Klugman, R. A. Bonomo, L. B. Rice, M. M. Wagener, J. G. McCormack, and V. L. Yu.** 2004. International prospective study of *Klebsiella pneumoniae* bacteremia: implications of extended-spectrum beta-lactamase production in nosocomial Infections. Ann. Intern. Med. **140:**26–32.
32. **Podschun, R., and U. Ullmann.** 1998. *Klebsiella* spp. as nosocomial pathogens: epidemiology, taxonomy, typing methods, and pathogenicity factors. Clin. Microbiol. Rev. **11:**589–603.
33. **Quah, B. J., and H. C. O'Neill.** 2005. Maturation of function in dendritic cells for tolerance and immunity. J. Cell Mol. Med. **9:**643–654.
34. **Regueiro, V., D. Moranta, M. A. Campos, J. Margareto, J. Garmendia, and J. A. Bengoechea.** 2009. *Klebsiella pneumoniae* increases the levels of Toll-like receptors 2 and 4 in human airway epithelial cells. Infect. Immun. **77:**714–724.
35. **Regueiro, V., M. A. Campos, J. Pons, S. Albertí, and J. A. Bengoechea.** 2006. The uptake of a *Klebsiella pneumoniae* capsule polysaccharide mutant triggers an inflammatory response by human airway epithelial cells. Microbiology **152:**555–566.
36. **Rescigno, M., M. Urbano, B. Valzasina, M. Francolini, G. Rotta, R. Bonasio, F. Granucci, J. P. Kraehenbuhl, and P. Ricciardi-Castagnoli.** 2001. Dendritic cells express tight junction proteins and penetrate gut epithelial monolayers to sample bacteria. Nat. Immunol. **2:**361–367.
37. **Sabatté, J., J. Maggini, K. Nahmod, M. M. Amaral, D. Martínez, G. Salamone, A. Ceballos, M. Giordano, M. Vermeulen, and J. Geffner.** 2007. Interplay of pathogens, cytokines and other stress signals in the regulation of dendritic cell function. Cytokine Growth Factor Rev. **18:**5–17.
38. **Sahly, H., I. Ofek, R. Podschun, H. Brade, Y. He, U. Ullmann, and E. Crouch.** 2002. Surfactant protein D binds selectively to *Klebsiella pneumoniae* lipopolysaccharides containing mannose-rich O-antigens. J. Immunol. **169:**3267–3274.
39. **Sahly, H., R. Podschun, T. A. Oelschlaeger, M. Greiwe, H. Parolis, D. Hasty, J. Kekow, U. Ullmann, I. Ofek, and S. Sela.** 2000. Capsule impedes adhesion to and invasion of epithelial cells by *Klebsiella pneumoniae*. Infect. Immun. **68:**6744–6749.
40. **Sallusto, F., and A. Lanzavecchia.** 1994. Efficient presentation of soluble antigen by cultured human dendritic cells is maintained by granulocyte/macrophage colony-stimulating factor plus interleukin 4 and downregulated by tumor necrosis factor alpha. J. Exp. Med. **179:**1109–1118.
41. **Tyrer, P., A. R. Foxwell, A. W. Cripps, M. A. Apicella, and J. M. Kyd.** 2006. Microbial pattern recognition receptors mediate M-cell uptake of a gram-negative bacterium. Infect. Immun. **74:**625–631.
42. **Underhill, D. M., and B. Gantner.** 2004. Integration of Toll-like receptor and phagocytic signaling for tailored immunity. Microbes Infect. **6:**1368–1373.
43. **van Kooyk, Y., and T. B. Geijtenbeek.** 2003. DC-SIGN: escape mechanism for pathogens. Nat. Rev. Immunol. **3:**697–709.
44. **von Garnier, C., and L. P. Nicod.** 2009. Immunology taught by lung dendritic cells. Swiss Med. Wkly. **139:**186–192.
45. **von Wulffen, W., M. Steinmueller, S. Herold, L. M. Marsh, P. Bulau, W. Seeger, T. Welte, J. Lohmeyer, and U. A. Maus.** 2007. Lung dendritic cells elicited by Fms-like tyrosine 3-kinase ligand amplify the lung inflammatory response to lipopolysaccharide. Am. J. Respir. Crit. Care Med. **176:**892–901.
46. **Wu, M. F., C. Y. Yang, T. L. Lin, J. T. Wang, F. L. Yang, S. H. Wu, B. S. Hu, T. Y. Chou, M. D. Tsai, C. H. Lin, and S. L. Hsieh.** 2009. Humoral immunity against capsule polysaccharide protects the host from magA+ *Klebsiella pneumoniae*-induced lethal disease by evading Toll-like receptor 4 signaling. Infect. Immun. **77:**615–621.
47. **Yoshida, K., T. Matsumoto, K. Tateda, K. Uchida, S. Tsujimoto, and K. Yamaguchi.** 2000. Role of bacterial capsule in local and systemic inflammatory responses of mice during pulmonary infection with *Klebsiella pneumoniae*. J. Med. Microbiol. **49:**1003–1010.
48. **Zhang, P., S. Snyder, P. Feng, P. Azadi, S. Zhang, S. Bulgheresi, K. E. Sanderson, J. He, J. Klena, and T. Chen.** 2006. Role of N-acetylglucosamine within core lipopolysaccharide of several species of gram-negative bacteria in targeting the DC-SIGN (CD209). J. Immunol. **177:**4002–4011.

Editor: A. J. Bäumler